



Pharmaceutical Nanotechnology

Interaction of biodegradable nanoparticles with intestinal cells: The effect of surface hydrophilicity

Marie Gaumet¹, Robert Gurny, Florence Delie^{*}

Department of Pharmaceutics and Biopharmaceutics, School of Pharmaceutical Sciences, University of Geneva, University of Lausanne, 30, Quai E. Ansermet, CH-1211 Geneva 4, Switzerland

ARTICLE INFO

Article history:

Received 22 December 2008

Received in revised form

21 September 2009

Accepted 3 October 2009

Available online 13 October 2009

Keywords:

Nanoparticles

Surface hydrophilicity

Fluorescence spectroscopy

Biodegradable polymers

Caco-2 cells

Chitosan

Cellular uptake

ABSTRACT

The aim of the present work was to study the influence of surface hydrophilicity of biodegradable polymeric nanoparticles on cellular uptake by Caco-2 cells. Poly(D,L-lactide-co-glycolide acid) particles loaded with a fluorescent dye, 3,3'-diocetadecyloxacarbo-cyanine perchlorate (DiO), were prepared by the emulsion–evaporation process. Three batches of particles with narrow size distribution (100, 300 and 1000 nm) were produced using selective centrifugation. One set of particles was coated by adsorption of chitosan to increase the hydrophilicity of the particles. The interaction of particles with Caco-2 cells was determined by fluorescence spectroscopy and the number of particles associated with one single cell was then calculated. Interaction with cells was clearly dependant on particle size and surface hydrophilicity. Particles in the range of 100 nm presented higher interaction when compared to larger particles. Approximately 6000 uncoated particles and more than 30,000 chitosan-coated particles were quantified per cell. Confocal microscopy confirmed the spectroscopic measurements and revealed the location of the particles in the cell monolayer. Only small particles were observed intracellularly, whereas particles larger than 300 nm were associated with the apical membranes. The location of particles <300 nm appeared to be intracellular and some particles colocalized with the nucleus.

© 2009 Elsevier B.V. All rights reserved.

1. Introduction

Particle size, the readily accessible parameter for characterizing particles, has been shown to be crucial regarding interaction with cells (Jani et al., 1990; Carr et al., 1996; Desai et al., 1997; McClean et al., 1998), since a smaller particle size is often correlated with a greater extent of uptake. Only a few studies have aimed to correlate cellular uptake with other particle properties, especially hydrophilicity. Hillery and Florence have observed in rats that the coating of polystyrene nanoparticles with poloxamer, which confers higher hydrophilicity, decreased the gastrointestinal uptake (Hillery and Florence, 1996). However, the increase in hydrophilicity was also correlated with a change in particle surface charge, from –30 to –19 mV, due to the presence of poloxamer. Win and Feng showed a significantly different cellular uptake between nanoparticles made with polymers of different hydrophilicities (Win and Feng, 2005). However, the surface charges of the two kinds of particles were not comparable, being –19 and

–37 mV. Therefore, the change in the rate of uptake could also be related to the variation of surface charge and not only to surface hydrophilicity. Coating with a hydrophilic compound often leads to a change in the particle preparation conditions, modifying then particle physico-chemical properties implicated in cellular uptake. The literature provides examples where the change of one parameter leads to the modification of the characteristics of the particles (Hillery and Florence, 1996; Behrens et al., 2002). Consequently, the influence of particle hydrophilicity on cellular uptake has not been studied carefully and independently of other parameters, such as charge. Finally, any certainty about the increase of the surface hydrophilicity cannot be achieved without a proper determination of the parameters that could be involved in cell interaction.

Preparation and characterization of biodegradable polymeric particles with well defined sizes (100, 300 and 1000 nm) and narrow distribution have been previously reported (Gaumet et al., 2007). The accurate surface property characterization showed similar zeta potential and hydrophilicity among the batches. 3,3'-diocetadecyloxacarbo-cyanine perchlorate (DiO) was incorporated as a fluorescent probe in the particles and its ability to remain in the matrix during *in vitro* experiments was investigated.

The first objective of this work was to prepare two sets of particles presenting the same size and charge, but differing in surface hydrophilicity. Due to its hydrophilic properties, chitosan was chosen as a coating agent to increase the surface hydrophilicity of the

^{*} Corresponding author. Tel.: +41 22 379 65 73; fax: +41 22 379 65 67.

E-mail address: Florence.delie@unige.ch (F. Delie).

¹ Current address: Department of Pharmaceutics, College of Pharmacy, Twin Cities Campus, University of Minnesota, 9-177 Weaver-Densford Hall, 308 Harvard St SE, Minneapolis, MN 55455, United States.

preformed biodegradable particles (Messai and Delair, 2005). Chitosan is a biocompatible polysaccharide extensively investigated for drug delivery applications (Agnihotri et al., 2004; Illum, 1998). Its structure is similar to cellulose and is positively charged at low pH but uncharged at neutral and basic pH. Chitosan is commonly characterized by its degree of deacetylation (DD) and its molecular weight (MW).

The second objective was to study the interaction of these particles with an *in vitro* model. Caco-2 cells, a human colon carcinoma cell line, commonly used as intestinal cell model for particle uptake studies (Delie and Rubas, 1997), were chosen. Quantitative aspects of the particle–cell interaction were studied by fluorescence spectroscopy and qualitative aspects through confocal microscopy.

2. Materials and methods

2.1. Materials

Particles were produced using a polyester, the poly(D,L-lactide-co-glycolide acid) (PLGA, Resomer® RG502, lactic to glycolic ratio 50:50, MW 12,000 Da), purchased from Boehringer-Ingelheim (Ingelheim, Germany). Polyvinylalcohol (PVAL, Mowiol® 4-88, MW 31,000 Da), used as surfactant, was obtained from Clariant GmbH (Frankfurt am Main, Germany). Chitosan with a MW of 160 kDa and a DD of 87% (Protasan® UP CL 110) was supplied by Pronova Biopolymer a.s. (Oslo, Norway) and used as the hydrophilic coating of the PLGA particles. The fluorescent dyes 3,3'-diiodo-4,4'-dimethoxydiphenylmethane (DiO, MW 882), Concanavalin A (Alexa Fluor® 594 conjugate) and Hoechst 33342 were purchased from Molecular Probes (Leiden, The Netherlands). Rose Bengal was obtained from Sigma Chemical Co. (St. Louis, MO, USA). Caco-2 cells were a gift from the Department of Genetics and Microbiology of the Centre Médico-Universitaire (University of Geneva, Switzerland). Hank's Balanced Salt Solution (HBSS), DMEM medium, non-essential amino acids, penicillin–streptomycin solution, Dulbecco's phosphate buffer solution (D-PBS), and trypsin–EDTA solution were purchased from Gibco (Invitrogen™ Life Technologies, AG, Basel, Switzerland). Foetal calf serum (FCS) was acquired from Brunschwig (Basel, Switzerland). The 6-well and 24-well plates were obtained from Costar® (Corning Inc., New York, NY, USA) and the glass cover slides from Erie Scientific Company (Portsmouth, NH, USA). Vectashield® (Vector Laboratories Inc., Burlingame, CA, USA) was used as the mounting medium for confocal microscopy.

2.2. Methods

2.2.1. Particle preparation

2.2.1.1. PLGA particles. Nanoparticles and microparticles were obtained by the emulsion–evaporation process (Gurny et al., 1981) followed by selective centrifugation for size separation. In brief, 1 ml of a solution containing 10% (w/v) PLGA and 0.01% (w/v) DiO in methylene chloride was poured into an aqueous solution of 1% PVAL (2 ml for nanoparticles and 20 ml for microparticles) to obtain an oil-in-water emulsion. For nanoparticle preparation, both phases were emulsified by sonication (S-450D®, Branson Ultrasonic S.A., Geneva, Switzerland) in an ice bath for 30 s using a 3 mm microtip probe sonicator set at 40 W of energy output. The emulsion was then poured dropwise into 50 ml of water and stirred for 1 h at 4 °C and 2 h at room temperature to allow solvent evaporation. For microparticle preparation, the emulsification was done using an ultra-homogenizer IKA®-Labortechnik Ultra-turrax T25 (Janke and Kunkel, Staufen, Germany) at a stirring rate of 20,500 rpm during

10 min in an ice bath. The emulsion was magnetically stirred for 12 h at room temperature to allow solvent evaporation. The particle suspensions were collected by selective centrifugation (Avanti® 30 Centrifuge, Beckman Coulter Inc., Fullerton, CA, USA) to separate out a given size population as detailed in Gaumet et al., 2007. In brief, decreasing the residual centrifuge force (RCF) allowed the collection of the large particles in the pellet and high RCF on the supernatant allowed the collection of the smallest ones. By changing the centrifugation time, the centrifugation becomes selective, allowing the acquisition of three batches of particles. A minimum of four centrifugation steps was applied to each batch to obtain the desired sizes and also to partially remove the surfactant. The particles were then kept in suspension, stored at 4 °C and used in the 10 following days for incubation experiments to avoid degradation.

2.2.1.2. Chitosan-PLGA particles. Hydrophilic particles were obtained from the PLGA particles previously described, by adding an aqueous solution of chitosan during the washing step. In the case of nanoparticles, they were suspended in 3 ml of 0.1% (w/v) Protasan®. After the third washing step, particles were resuspended and stirred for 10 min before the last wash. In the case of microparticles, 5 ml of 0.1% (w/v) Protasan® were added to the aqueous phase of PVAL. Three batches of PLGA particles coated with a thin layer of chitosan were obtained without significantly modifying their size. Each particle batch was prepared in triplicate. The particles were then kept in suspension, stored at 4 °C and used in the 2 following days for incubation experiments to avoid degradation and chitosan desorption.

2.2.2. Size characterization

2.2.2.1. Light scattering. Mean size, size distribution and polydispersity index (PI) were obtained by dynamic light scattering (DLS) using a Zetasizer® 3000HS (Malvern Instruments, Malvern, UK) at a 90° scattering angle, at room temperature in Milli-Q® water, and recorded for a duration determined by the zetasizer program in the automatic mode.

2.2.2.2. Scanning electron microscopy. Particles were diluted in distilled water, dropped onto stubs, air dried, covered by a 5–20 nm thick layer of gold or platinum and then examined by scanning electron microscopy (SEM), using a JSM-6300® (JEOL, Tokyo, Japan) or a Philips® XL-30 (Philips, Lancashire, UK). The mean particle size was analysed from SEM pictures using the ImageJ® software (U.S. National Institutes of Health, Bethesda, MA, USA) on at least 200 particles to compare with the results obtained by DLS.

2.2.3. Surface characterization

2.2.3.1. Charge. Zeta potential measurements, directly related to the surface charge density, were determined by electrophoretic mobility on particle suspensions in Milli-Q® water at pH 7 and room temperature using the aqueous flow cell in the automatic mode of the Zetasizer® 3000HS based on Helmholtz–Smoluchowski's equation (Malvern Instruments, Malvern, UK).

2.2.3.2. Hydrophilicity. Surface hydrophilicity was quantified by measuring the adsorption of the hydrophilic dye Rose Bengal (RB) onto the particles, as previously described. The aqueous phase and the surface of the particles are considered as two phases between which RB partitions (Müller, 1991). Briefly, particles in suspension in RB aqueous solutions at different concentrations (from 2 to 75 µg/ml) were vortexed for 3 h at room temperature. After centrifugation, the RB concentration in the supernatant was determined by spectrometry at 548 nm (Safire®, Tecan, Salzburg, Austria). The amount of RB adsorbed on the particle surface was

Table 1

Physico-chemical properties of the PLGA and Ch-PLGA particles.

Batch	Mean size (nm)		Polydispersity index	Zeta potential (mV)	Hydrophilicity H (10^{-10} g/m ²)	Residual PVAL (% w/w)
	DLS ^a	SEM ^b				
PLGA ₁₀₀	168 ± 10	99 ± 10	0.08 ± 0.01	−10.4 ± 2.8	5.8 ± 1.0	3.4
Ch-PLGA ₁₀₀	182 ± 11	87 ± 12	0.08 ± 0.03	−4.7 ± 2.7	19.9 ± 1.6	± 0.8
PLGA ₃₀₀	301 ± 9	229 ± 40	0.06 ± 0.02	−11.1 ± 1.3	4.7 ± 0.5	2.3
Ch-PLGA ₃₀₀	330 ± 6	244 ± 33	0.07 ± 0.00	−3.9 ± 3.2	15.9 ± 1.0	± 0.8
PLGA ₁₀₀₀	1124 ± 91	716 ± 130	0.07 ± 0.02	−12.1 ± 0.1	5.7 ± 1.2	1.3
Ch-PLGA ₁₀₀₀	1142 ± 78	998 ± 124	0.09 ± 0.03	−8.4 ± 5.5	16.8 ± 0.5	± 0.4

 $n = 3 \pm \text{SD}$.^a Dynamic light scattering.^b Scanning electron microscope, $n = 200$ particles \pm SD.

then calculated by difference. The parameter H (10^{-10} g/m²) which represents the amount of RB bound per surface of the particles, was calculated from Eq. (1) as follows:

$$H = \frac{0.01Ndr}{3} \quad (1)$$

where N is the maximum amount of RB bound per mass of particles ($\mu\text{g}/\text{mg}$); d is the particle density ($1.06 \text{ g}/\text{cm}^3$), and r is the particle radius (nm).

2.2.3.3. Residual surfactant determination. The percentage of residual surfactant was measured by a colorimetric assay based on the formation of a complex of iodine-PVAL in the presence of boric acid which was analysed at 635 nm (Sakurada, 1985).

2.2.4. DiO incorporation

The amount of DiO incorporated was determined by spectrofluorimetry (fluorescence spectra in methylene chloride: $\lambda_{\text{ex}}/\lambda_{\text{em}} = 489 \text{ nm}/506 \text{ nm}$) after particle solubilization in methylene chloride (1 mg/ml).

2.2.5. Cell culture

The Caco-2 cells were cultured in flasks and trypsinized at 80% confluence according to a standard protocol (Pietzonka et al., 2002). Cells were seeded at a density of 25,000 cells/cm² either in 24-well plates for quantitative experiments or on cover slides placed in 6-well plates for confocal microscopy. Cells were grown at 37 °C in an atmosphere of 5% CO₂, using DMEM culture medium supplemented with 10% FCS, 1% non-essential amino acids and 1% of penicillin and streptomycin. Cells were grown for at least 10 days after the confluence, while the medium was changed every other day. The cells were used between passage 10 and 15 to limit the alteration of their properties associated with high passage number (Bailey et al., 1996).

2.2.6. Particle interaction study

2.2.6.1. Incubation experiments. The culture medium was removed and the cells were washed three times with HBSS. After 30 min of equilibration, HBSS was replaced by 500 μl of particle suspension in HBSS at 37 °C (100, 500, 1000 and 2000 $\mu\text{g}/\text{well}$). The incubation was performed for 4 h at 37 °C in an atmosphere of 5% CO₂. At the end of the experiment, the suspensions were removed and the cells

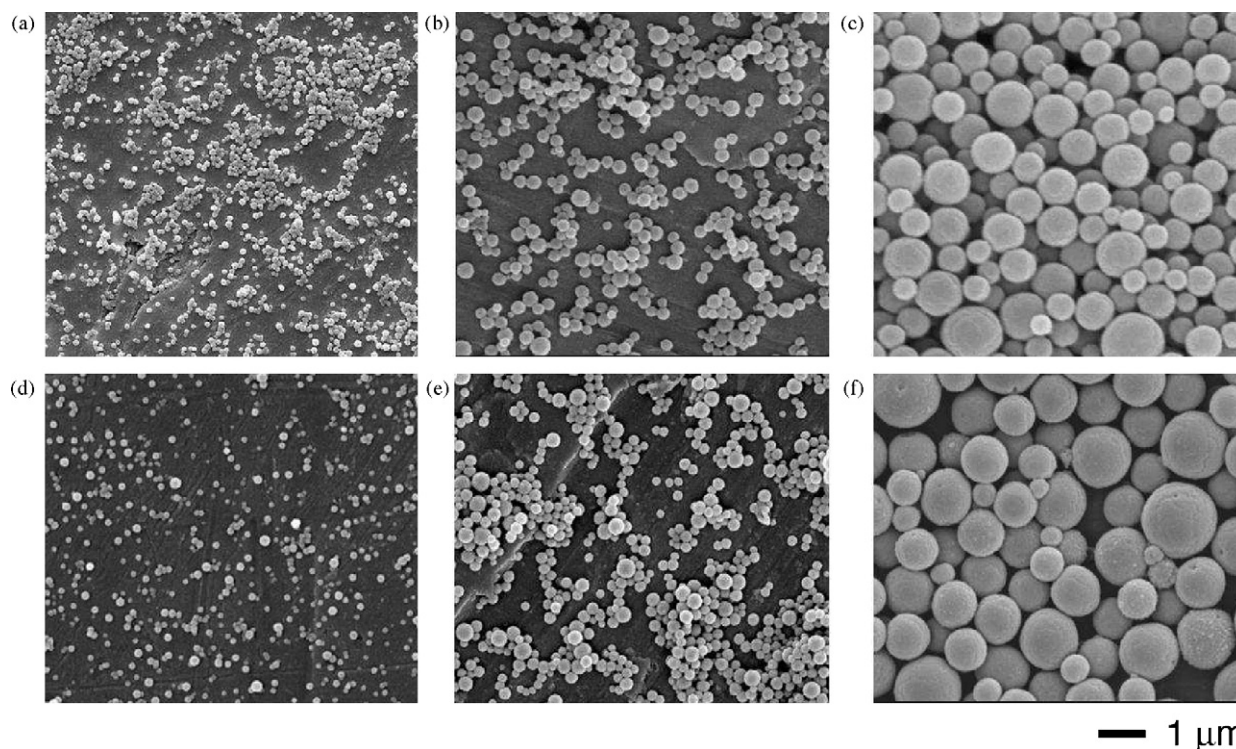


Fig. 1. Scanning electron micrograph of the particles. (a) PLGA₁₀₀, (b) PLGA₃₀₀, (c) PLGA₁₀₀₀, (d) Ch-PLGA₁₀₀, (e) Ch-PLGA₃₀₀, and (f) Ch-PLGA₁₀₀₀. The six batches are presented at the same magnification (10,000 \times).

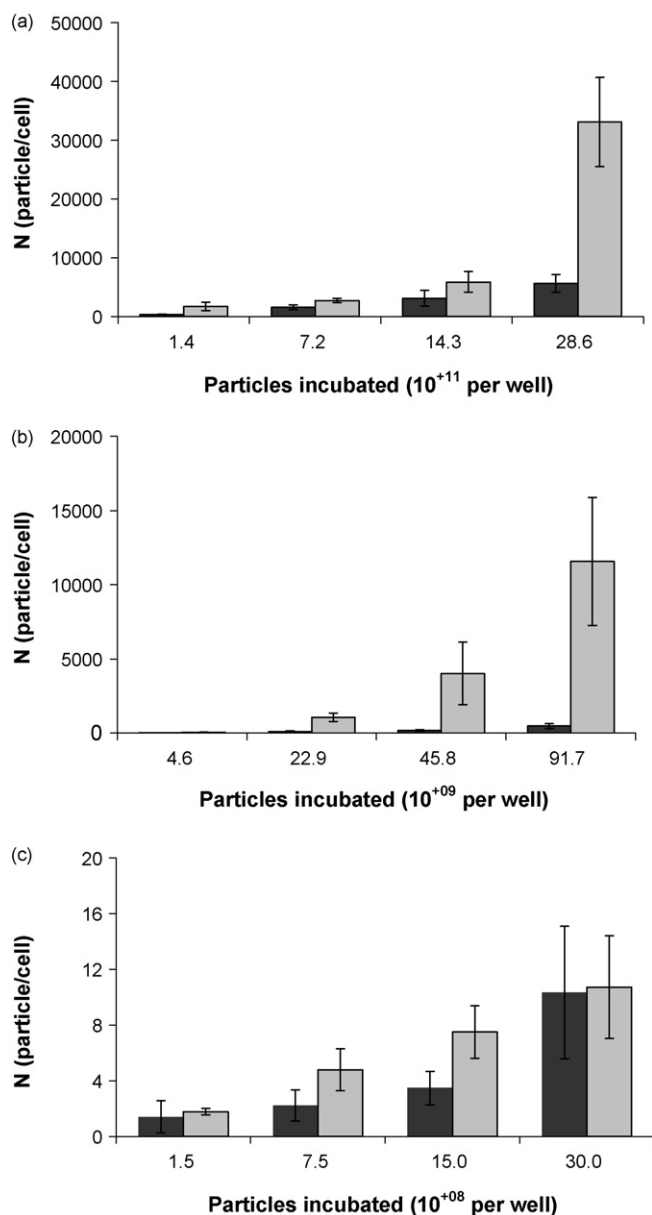


Fig. 2. Interaction between Caco-2 cells and particles of PLGA and Ch-PLGA. (■) PLGA series, (□) Ch-PLGA series, (a) PLGA₁₀₀ and Ch-PLGA₁₀₀, (b) PLGA₃₀₀ and Ch-PLGA₃₀₀, and (c) PLGA₁₀₀₀ and Ch-PLGA₁₀₀₀.

were washed 4 times with HBSS to remove particles that had not interacted with cells.

2.2.6.2. Fluorescence spectroscopy. The fluorescence associated with the cells was recorded with a microplate reader (Safire®, Tecan, Salzburg, Austria) set to $\lambda_{ex} = 485$ nm and $\lambda_{em} = 505$ nm. The integration time was 20 μ s and 12 points per well were read in circle mode. The bandwidths and the gain detection were adapted for each assay to optimize the signal. The fluorescence of each well was measured three times to calculate the percentage of particles interacting with the cells. A first reading was made before adding the particles to determine the background signal of the cells (S_c) in HBSS. A second reading was performed after the particle suspension was added (S_p). Finally, the last one was performed after washing (S_i). Eq. (2) was used to calculate the percentage of interaction (P_i):

$$P_i = \frac{S_i - S_c}{S_p - S_c} \times 100 \quad (2)$$

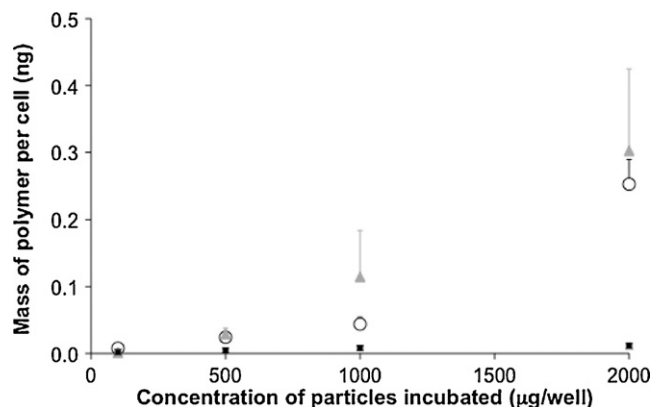


Fig. 3. Interaction between Ch-PLGA particles and Caco-2 cells expressed as mass of polymer per cell. (○) Ch-PLGA₁₀₀, (△) Ch-PLGA₃₀₀, and (■) Ch-PLGA₁₀₀₀.

The linearity of correlation signal versus particle amount has been checked (data not shown). P_i was accurately calculated for each reading point and was not obtained using the means of the 12 reading points of S_c , S_p and S_i .

As the fluorescence signal is proportional to the amount of particles in one well, the P_i is related to the mass of particles remaining within the cell layer after washing steps. M (μ g), the mass of particles remaining per well can be calculated according to Eq. (3):

$$M = \frac{P_i Q}{100} \quad (3)$$

where Q is the mass of particles added per well (μ g). After counting the cells, N , the number of particles having interacted per cell is determined (Eq. (4)):

$$N = \frac{P_i C}{d(4/3)\pi(D/2)^3 n \times 10^{-13}} \quad (4)$$

where d is the particle density, D is the diameter of particles given by DLS for each batch and n is the number of the cells per well counted after each experiment (3 wells counted in each 24-well plate). The batches of PLGA and Chitosan-PLGA particles, prepared in triplicate, were tested in 5 wells, which correspond to 15 samples for one concentration of particles.

2.2.6.3. Confocal microscopy. To localize the particles in the cell monolayer, cell apical membranes were stained with Concanavalin A and Alexa Fluor® 594 conjugate and the nuclei were stained with Hoechst 33342. Cells were fixed with an aqueous solution of 8% (v/v) formaldehyde before applying the mounting medium. Cells were observed with a confocal laser scanning microscope CLSM 510 Meta (Zeiss AG, Zurich, Switzerland) equipped with a diode at 405 nm of excitation, an Argon laser (providing the excitation at 488 nm) and a helium/neon laser (providing the excitation at 543 nm). An oil immersion objective (100 \times) was used. Images were processed with the Imaris® software, 3D multichannel image processing software for confocal microscopic images (Bitplane AG, Zurich, Switzerland).

2.2.6.4. Trypan blue test exclusion. Cell viability was checked by a Trypan blue exclusion test (Torres-Lugo et al., 2002). This assay has been performed with 100 and 1000 nm particles at the concentration of 2000 μ g/well. After incubation with particles, cell monolayers were rinsed three times with PBS and trypsinized to resuspend the cells. Then, cells were treated with 100 μ l of a 0.4% Trypan blue dye solution and counted with a Neubauer hemocytometer. Cells appearing blue were considered dead whereas viable cells excluded the dye.

3. Results

3.1. Particle physico-chemical characterization

The properties of the two sets of PLGA and Chitosan-PLGA (Ch-PLGA) particles are listed in Table 1. Three batches of nanoparticles with a size close to 100, 300 and 1000 nm were produced. For all of the batches, low PI values (between 0.06 and 0.09) were confirmed by electron microscopy observations (Fig. 1). All the particles were negatively charged between -4 and -12 mV at pH 7. Size did not influence the hydrophilicity of the particles and values of approximately $5 \times 10^{-10} \mu\text{g}/\mu\text{m}^2$ and $18 \times 10^{-10} \mu\text{g}/\mu\text{m}^2$ were found for PLGA and Ch-PLGA particles, respectively. The residual amount of PVAL was comparable between all of the batches (1–3%, w/w). Regarding DiO loading, an average of $9.3 \pm 0.4 \times 10^{-4}\%$ (mass of DiO per mass of PLGA) was incorporated, which represents incorporation efficiencies above 90%.

3.2. Particle interaction with cells

3.2.1. Fluorescence spectroscopy

Fig. 2 presents the interaction data of PLGA and Ch-PLGA particles with Caco-2 cells expressed as N , the number of particles associated with one cell, as a function of particle concentration. An increase in the number of particles associated with one cell was observed when the amount of incubated particles increased. The 100 nm particles present a high extent of interaction compared to the other sizes with more than 6000 particles per cell for PLGA₁₀₀ and over 30,000 for Ch-PLGA₁₀₀. For the 1000 nm particles, N drops to 10 and 11 particles per cell for PLGA₁₀₀₀ and Ch-PLGA₁₀₀₀, respectively. Data has been also expressed as mass of particles per cell has for the Ch-PLGA particles (Fig. 3).

3.2.2. Confocal microscopy

Confocal microscopy images show the actual association of PLGA (Fig. 4a–c) and Ch-PLGA (Fig. 4d–f) particles with Caco-2 cells.

The size dependency is clearly seen on these images. The higher affinity of Ch-PLGA particles to Caco-2 cells compared to PLGA particles is also observed, except in the case of the 1000 nm particles, where no difference can be seen (Fig. 4c and f). Orthogonal sections show that the particles of PLGA₃₀₀, Ch-PLGA₃₀₀, PLGA₁₀₀₀ and Ch-PLGA₁₀₀₀ (Fig. 4b, c, e and f) are associated with the cell membrane whereas PLGA₁₀₀, Ch-PLGA₁₀₀ and Ch-PLGA₃₀₀ appear to be more intracellular or even nuclear. Nuclear staining with Hoechst 33342 confirmed the localization of PLGA₁₀₀ and Ch-PLGA₁₀₀ in the nuclei (Fig. 5a and b).

3.2.3. Cell viability

The trypan blue exclusion test revealed more than 95% cell viability for all of the tested batches.

4. Discussion

In the field of oral administration of nanoparticles, size and charge are considered to be critical parameters for the ability to cross the intestinal barrier (Tabata et al., 1996). Several studies have been conducted with nanoparticles of around 300 nm and suggested that negatively charged particles may interact better with enterocytes (Dong and Feng, 2005; des Rieux et al., 2005; Win and Feng, 2005; Mathiowitz et al., 1997; Kriwet and Kissel, 1996; Hillery and Florence, 1996). However, the influence of surface hydrophilicity is rarely investigated. Some studies used the coating of nanoparticles with polymers of different hydrophilic–lipophilic balance (Eldridge et al., 1990; Russell-Jones et al., 1999; Behrens et al., 2002), but surface hydrophilicity of the particles is seldom measured, most likely because of the difficulty in assessing this parameter. Without a proper characterization of surface hydrophilicity it is difficult to ascertain the role of this parameter on intestinal absorption (Win and Feng, 2005). Furthermore, change in particle hydrophilicity is frequently associated to the variation of other parameters such as charge (Hillery and Florence, 1996; Behrens et al., 2002). Consequently, the aim of the present study was to prepare par-

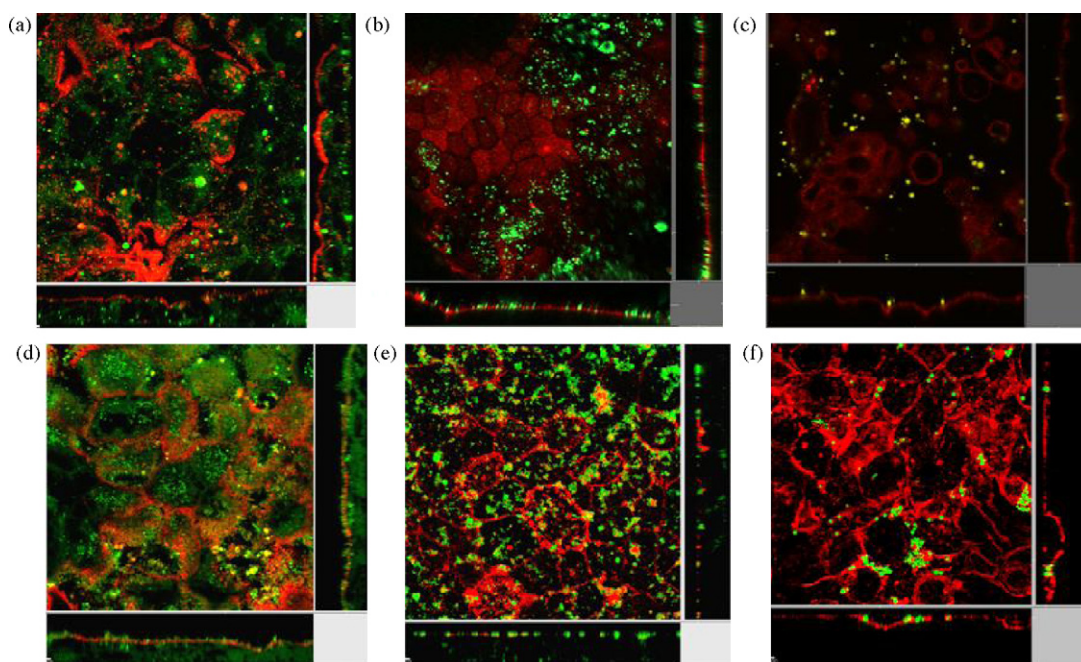


Fig. 4. Localization of PLGA and Ch-PLGA particles within intestinal cells. Confocal microscopy images of Caco-2 cells after 4 h incubation with particles (2 mg per well). The confocal micrographs represent three-dimensional analysis of the optical sections (z-axis) of the cell monolayer. Red: apical membrane stained with Alexa red-Concanavalin A; green: particles. (a) PLGA₁₀₀, (b) PLGA₃₀₀, (c) PLGA₁₀₀₀, (d) Ch-PLGA₁₀₀, (e) Ch-PLGA₃₀₀, and (f) Ch-PLGA₁₀₀₀. (For interpretation of the references to color in this figure legend, the reader is referred to the web version of the article.)

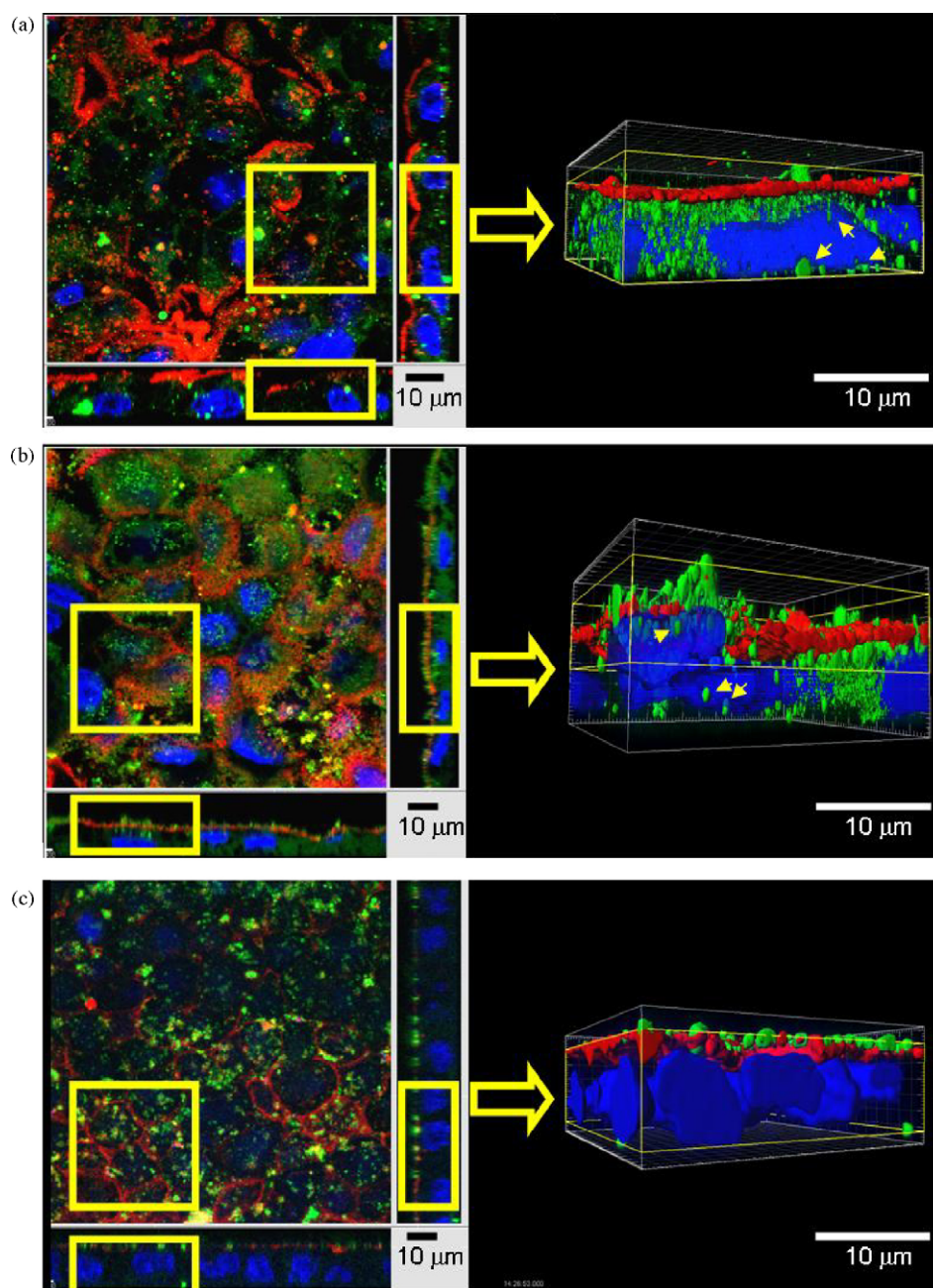


Fig. 5. Intracellular localization of PLGA and Ch-PLGA particles within intestinal cells. Confocal microscopy images of Caco-2 cells after 4 h incubation with particles (2000 $\mu\text{g}/\text{well}$). The confocal micrographs on the left represent three-dimensional analysis of the optical sections (z-axis) of the cell monolayer, whereas an area has been treated by the Imaris software, on the right. Red: apical membrane, stained with Alexa red-Concanavalin A; green: particles. Blue: nuclei died with Hoechst 33342. (a) PLGA₁₀₀, (b) Ch-PLGA₁₀₀, and (c) Ch-PLGA₃₀₀. Yellow arrow indicates the presence of nanoparticles within the nucleus. (For interpretation of the references to color in this figure legend, the reader is referred to the web version of the article.)

ticles that differ only in the hydrophilicity to further quantify interaction with Caco-2 cells. The number of particles that interacted with one cell was determined by a previously reported fluorescence spectroscopy method (Gaumet et al., 2009). The localization of particles within the cells was assessed by confocal microscopy.

To prepare more hydrophilic particles without changing the charge, a low amount of chitosan was adsorbed on the surface of PLGA particles. Protasan® has been chosen because of its high DD, as recommended by Messai and Delair who have investigated the critical parameters for the design of chitosan-coated poly(lactic acid) particles (Messai and Delair, 2005). They

also demonstrated that the adsorption of chitosan was spontaneous. On the other hand, chitosan desorption was significant after 10 days of storage. Therefore, our particles were used less than 2 days after preparation. A low MW was preferred to avoid the formation of a thick and dense coating onto the PLGA particles to keep the size similar to the uncoated particles. Protasan® also has the advantage of being soluble in water at neutral pH, which avoids, such as acetic acid, for solubilization. Indeed, variations of certain conditions, such as pH, during the preparation steps may change the physico-chemical properties of the resulting particles. We assumed that the formation of an ion pair occurred between the aminated functionalities of

the chitosan and the hydroxylic functionalities of the PVAL. We observed the rapid adsorption of chitosan onto the PLGA particles, which supports the hypothesis developed by Messai and Delair (2005).

In this study, narrow size distributions were demonstrated for all batches (Table 1). The very low amount of chitosan (0.1%, w/v) did not significantly influence particle size, PI, or charge (Table 1, Fig. 1). Zeta potentials of Protasan®-coated particles were measured at different pHs (data not shown). As reported in the literature (Messai and Delair, 2005), a decrease in the zeta potential with a decrease of the pH with a charge inversion at pH 6 was observed. Thus, above pH 6.5, the pH at which the assays with cells were run, the amino groups of the chitosan, responsible for the positive charges, were neutralized and both coated and uncoated particles were negatively charged as attested by the zeta potential data (Table 1).

The majority of the reports studying the relationship between particle physico-chemical properties and cellular uptake compare the therapeutic efficiency or the percentage of internalization of particles (Tabata et al., 1996; Mitra et al., 2001; Dong and Feng, 2005). However, the number of particles interacting with each cell is rarely evaluated. This approach nevertheless allows for a more accurate comparison between PLGA and Ch-PLGA nanoparticles, because the exact particle diameter and the number of intestinal cells were taken into account for each experiment. In terms of the number of particles per cell, more Ch-PLGA nanoparticles interacted with cells than for PLGA nanoparticles (Fig. 2a and b). It appears clearly that the increase in *N* as function of the concentration is linear for the PLGA nanoparticles whereas it is exponential for the Ch-PLGA nanoparticles. Regarding the 1 μ m particles, the difference of *N* is not significant between the uncoated and coated particles (Fig. 2c).

The calculation of the number of particles per cell allowed to apprehend the effect of the hydrophilicity on the cell–particle interaction. The present study demonstrates that the higher surface hydrophilicity is correlated with a larger interaction. However, the limiting factor remains the particle size because no significant improvement was observed with hydrophilic particles of 1 μ m. If the mass of particles per cell is considered for the Ch-PLGA particles instead of the number of particles per cell, particles of 300 nm appeared as efficient as the 100 nm particles (Fig. 3). From a therapeutic view point, these 300 nm particles might be more interesting since more polymer can be brought to the cell, potentially more drug is taken up.

After incubation with particles, Caco-2 monolayers were observed with CLSM. Confocal microscopy confirmed the results obtained with the microplate reader, showing a higher number of nanoparticles associated with cells compared to microparticles (Fig. 4). The majority of the PLGA₃₀₀ nanoparticles were associated with the apical cell membrane whereas the majority of PLGA₁₀₀ and Ch-PLGA₁₀₀ were found inside the cells (Fig. 4a, d and e). A small amount of Ch-PLGA₃₀₀ is observed intracellularly as well. A higher surface hydrophilicity favoured the penetration of 300 nm particles in the cytoplasm (Fig. 5c). The nuclear and cytoplasmic localizations of the smallest biodegradable particles (PLGA₁₀₀ and Ch-PLGA₁₀₀) were visualized by nuclear staining (Fig. 5a–c).

The methodology performed in the present study with biodegradable particle models, with narrow size distributions and comparable surface charges, demonstrated that among the studied particles, the negatively charged 100 or 300 nm particles that presented a high hydrophilicity appear to be the best candidates to target intestinal cells.

To summarize, hydrophilic particles were obtained by generating a thin coating of PLGA particles with chitosan without affecting either size or charge. These particles allowed the study of the influ-

ence of hydrophilicity on the cellular uptake independently of other parameters. The present study illustrates the potential of PLGA particles to interact with intestinal cells. The highest interaction level was correlated with the smallest size, the highest concentration and the highest hydrophilicity of particles. Furthermore, the observation of PLGA and Ch-PLGA nanoparticles in the nuclei of the Caco-2 cells suggests that such carriers can be used for targeting either the cell membrane or the cell nuclei, depending on their size. Surface hydrophilicity was found to be a determining factor for nanoparticle uptake. However, no correlation between hydrophilicity and interaction was noticed for particles measuring 1 μ m.

References

- Agnihotri, S.A., Mallikarjuna, N.N., Aminabhavi, T.M., 2004. Recent advances on chitosan-based micro- and nanoparticles in drug delivery. *J. Control. Release* 100, 5–28.
- Bailey, C.A., Bryla, P., Malick, A.W., 1996. The use of intestinal epithelial cell culture model. Caco-2, in pharmaceutical development. *Adv. Drug Deliv. Rev.* 22, 85–103.
- Behrens, I., Pena, A.I., Alonso, M.J., Kissel, T., 2002. Comparative uptake studies of bioadhesive and non-bioadhesive nanoparticles in human intestinal cell lines and rats: the effect of mucus on particle adsorption and transport. *Pharm. Res.* 19, 1185–1193.
- Carr, K.E., Hazzard, R.A., Reid, S., Hodges, G.M., 1996. The effect of size on uptake of orally administered latex microparticles in the small intestine and transport to mesenteric lymph nodes. *Pharm. Res.* 13, 1205–1209.
- Delie, F., Rubas, W., 1997. A human colonic cell line sharing similarities with enterocytes as a model to examine oral absorption: advantages and limitations of the Caco-2 model. *Crit. Rev. Ther. Drug Carrier Syst.* 14, 221–286.
- des Rieux, A., Ragnarsson, E.G., Gullberg, E., Preat, V., Schneider, Y.J., Artursson, P., 2005. Transport of nanoparticles across an in vitro model of the human intestinal follicle associated epithelium. *Eur. J. Pharm. Sci.* 25, 455–465.
- Desai, M.P., Labhasetwar, V., Walter, E., Levy, R.J., Amidon, G.L., 1997. The mechanism of uptake of biodegradable microparticles in Caco-2 cells is size dependent. *Pharm. Res.* 14, 1568–1573.
- Dong, Y., Feng, S.S., 2005. Poly(D,L-lactide-co-glycolide)/montmorillonite nanoparticles for oral delivery of anticancer drugs. *Biomaterials* 26, 6068–6076.
- Eldridge, J.H., Hammond, C.J., Meulbroek, J.A., Staas, J.K., Gilley, R.M., Tice, T.R., 1990. Controlled vaccine release in the gut-associated lymphoid tissues. I. Orally administered biodegradable microspheres target the Peyer's patches. *J. Control. Release* 11, 205–214.
- Gaumet, M., Gurny, R., Delie, F., 2007. Fluorescent biodegradable PLGA particles with narrow size distributions: preparation by means of selective centrifugation. *Int. J. Pharm.* 342, 222–230.
- Gaumet, M., Gurny, R., Delie, F., 2009. Localization and quantification of biodegradable particles in an intestinal cell model: the influence of particle size. *Eur. J. Pharm. Sci.* 36, 465–473.
- Gurny, R., Peppas, N.A., Harrington, D.D., Banker, G.S., 1981. Development of biodegradable and injectable latices for controlled release of potent drugs. *Drug Dev. Ind. Pharm.* 7, 1–25.
- Hillery, A.M., Florence, A.T., 1996. The effect of adsorbed poloxamer 188 and 407 surfactants on the intestinal uptake of 60-nm polystyrene particles after oral administration in the rat. *Int. J. Pharm.* 132, 123–130.
- Illum, L., 1998. Chitosan and its use as a pharmaceutical excipient. *Pharm. Res.* 15, 1326–1331.
- Jani, P., Halbert, G.W., Langridge, J., Florence, A.T., 1990. Nanoparticle uptake by the rat gastrointestinal mucosa: quantitation and particle size dependency. *J. Pharm. Pharmacol.* 42, 821–826.
- Kriwet, B., Kissel, T., 1996. Poly(acrylic acid) microparticles widen the intercellular spaces of caco-2 cell monolayers: an examination by confocal laser scanning microscopy. *Eur. J. Pharm. Biopharm.* 42, 233–240.
- Mathiowitz, E., Jacob, J.S., Jong, Y.S., Carino, G.P., Chickering, D.E., Chaturvedi, P., Santos, C.A., Vijayaraghavan, K., Montgomery, S., Bassett, M., Morrell, C., 1997. Biologically erodible microspheres as potential oral drug delivery systems. *Nature* 386, 410–414.
- McClean, S., Prosser, E., Meehan, E., O'Malley, D., Clarke, N., Ramtoola, Z., Brayden, D., 1998. Binding and uptake of biodegradable poly-DL-lactide micro- and nanoparticles in intestinal epithelia. *Eur. J. Pharm. Sci.* 6, 153–163.
- Messai, I., Delair, T., 2005. Adsorption of chitosan onto poly(D,L-lactic acid) particles: a physico-chemical investigation. *Macromol. Chem. Phys.* 206, 1665–1674.
- Mitra, S., Gaur, U., Ghosh, P.C., Maitra, A.N., 2001. Tumour targeted delivery of encapsulated dextran–doxorubicin conjugate using chitosan nanoparticles as carrier. *J. Control. Release* 74, 317–323.
- Müller, R.H., 1991. In: Müller, R.H. (Ed.), *Surface Hydrophobicity*. CRC Press, Boca Raton, pp. 99–109.
- Pietzonka, P., Rothen-Rutishauser, B., Langguth, P., Wunderli-Allenspach, H., Walter, E., Merkle, H.P., 2002. Transfer of lipophilic markers from PLGA and polystyrene nanoparticles to caco-2 monolayers mimics particle uptake. *Pharm. Res.* 19, 595–601.

- Russell-Jones, G.J., Veitch, H., Arthur, L., 1999. Lectin-mediated transport of nanoparticles across Caco-2 and OK cells. *Int. J. Pharm.* 190, 165–174.
- Sakurada, I., 1985. In: Menachem, L. (Ed.), *Chemical Reactions of Polyvinyl Alcohol*, vol. 6. Marcel Dekker, New York, pp. 137–159.
- Tabata, Y., Inoue, Y., Ikada, Y., 1996. Size effect on systemic and mucosal immune responses induced by oral administration of biodegradable microspheres. *Vaccine* 14, 1677–1685.
- Torres-Lugo, M., Garcia, M., Record, R., Peppas, N.A., 2002. Physicochemical behavior and cytotoxic effects of p(methacrylic acid-g-ethylene glycol) nanospheres for oral delivery of proteins. *J. Control. Release* 80, 197–205.
- Win, K.Y., Feng, S.S., 2005. Effects of particle size and surface coating on cellular uptake of polymeric nanoparticles for oral delivery of anticancer drugs. *Biomaterials* 26, 2713–2722.